Resonance Raman and Infrared Spectra of Molecular Oxygen Adducts of *N,N'*-Ethylenebis(2,2-diacetylethylideneaminato)cobalt(II)

K. Nakamoto,* Y. Nonaka, T. Ishiguro, M. W. Urban, M. Suzuki, M. Kozuka, Y. Nishida, and S. Kida

Contribution from the Todd Wehr Chemistry Building, Marquette University, Milwaukee, Wisconsin 53233, and the Department of Chemistry, Faculty of Science, Kyushu University, Fukuoka 812, Japan. *Received August 28, 1981*

Abstract: The infrared spectrum of base-free Co(J-en)O_2 (H_2(J-en) = *N,N'*-ethylenebis(2,2-diacetylethylideneamine)) was measured by using matrix cocondensation techniques. Its O_2 stretching frequency, $\nu(O_2)$, at 1260 cm^{-1} is much higher than that of Co(acacen)O_2 (H_2(acacen) *N,N'*-ethylenebis(acetylacetone imine)) at 1146 cm^{-1}. This high-frequency shift is attributed to the electron-withdrawing effect of the acetyl groups in Co(J-en) which results in a much less negatively charged O_2 relative to that of Co(acacen)O_2. Resonance Raman spectra of the O_2 adducts of Co(J-en) in solution were obtained and studied as a function of the nature of the axial ligand, solvent polarity, temperature, and O_2 pressure. The $\nu(O_2)$ of the 1:1 and 1:2 (O_2/Co) adducts were located in the regions 1150-1130 and 880-820 cm^{-1}, respectively, by $^{16}O_2$-$^{18}O_2$ substitution. The following conclusions have been obtained by using these $\nu(O_2)$ as the marker bands: (1) Formation of the 1:1 adduct is favored with a stronger base (axial ligand), in a more polar solvent, at lower temperature, and under higher O_2 pressure. (2) The $\nu(O_2)$ of the 1:2 adduct decreases linearly as the pK_a of the axial ligand increases. Different linear relationships are obtained, however, depending upon whether the ligand is a pure σ donor, π as well as σ donor, or π acceptor. The 1:2 adduct, $[Co(J\text{-}en)(py)]_2O_2$, and its $^{18}O_2$ analogue have been isolated as crystals and their $\nu(O_2)$ and ν_s(CoO) (symmetric stretch) assigned at 834 and 562 cm^{-1}, respectively. The Co-O_2 CT bands of the 1:1 and 1:2 adducts in solution equilibria (*n*-butylamine as the axial ligand) were located at ca. 550 and 610 nm, respectively, via excitation profile studies of their $\nu(O_2)$ vibrations. Possible origins of these CT bands are discussed in terms of rudimentary MO schemes.

To study the effects of the in-plane (L) and axial (B) ligands on the stability of the Co(L)(B)O_2 type adduct, Carter et al.[1] measured the equilibrium constant of the reaction Co(L)(B) + $O_2 \rightleftharpoons$ Co(L)(B)O_2 and the anodic potential of the Co(L)(B) type complex. Here Co(L) represents a series of Schiff base chelates such as shown below, and B denotes a variety of base ligands such as pyridine (py) and *n*-butylamine.

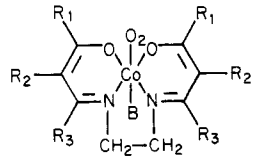

acacen, $R_1 = R_3 = CH_3$; $R_2 = H$
Phacacen, $R_1 = R_3 = CH_3$; $R_2 = C_6H_5$
Meacacen, $R_1 = R_2 = R_3 = CH_3$
bzacen, $R_1 = C_6H_5$; $R_2 = H$; $R_3 = CH_3$

They noted that the equilibrium constant increases linearly as the anodic potential increases in the Co(bzacen)B as well as in Co(L)(py) series. Since the anodic potential is a measure of the electron density on cobalt, their results suggested that the oxygen affinity increases as L or B donates more electrons to the metal.

Previously, we have shown that the $\nu(O_2)$ (O_2 stretching frequency) of an O_2 adduct of a Co(II) chelate is sensitive to the nature of both in-plane and axial ligands; the $\nu(O_2)$ of "base-free" Co(TPP)O_2 which is found at 1278 cm^{-1} [2] (H_2(TPP) = tetraphenylporphyrin), shifts to 1146 cm^{-1} when TPP is replaced by acacen[3] and to 1142 cm^{-1} when 1-methylimidazole (1-MeIm) coordinates to its axial position.[4]

N,N'-Ethylenebis(2,2-diacetylethylideneaminato)cobalt(II) (R_1 = CH_3, R_2 = $COCH_3$, and R_3 = H, abbreviated as Co(J-en)) is unique among the Schiff base complexes because it possesses electron-withdrawing acetyl groups as peripheral substituents. Kubokura et al.[5] have concluded that it is the presence of these acetyl groups in Co(J-en) that is responsible for the reversibility of oxygenation at room temperature and the appearance of visible bands upon oxygenation. Their conclusion is supported by ^{13}C NMR and electronic spectral studies and anodic potential measurements on a series of Ni(L) type complexes including Ni(J-en). This paper reports the infrared (IR) spectra of "base-free" Co(J-en)O_2 in argon matrices and the resonance Raman (RR) spectra of $[Co(J\text{-}en)(py)]_2O_2$ in the solid state as well as Co(J-en)(B)O_2 and $[Co(J\text{-}en)(B)]_2O_2$ in solution equilibria.

Experimental Section

Compounds. The complex Co(J-en) was prepared according to the literature method.[5] The 1:2 adduct, $[Co(J\text{-}en)(py)]_2O_2$, was obtained by dissolving Co(J-en) in toluene containing 5% py and bubbling oxygen or air through the solution until black-purple prismatic crystals were separated. Anal. Calcd for $C_{38}H_{46}O_{10}N_6(Co)_2$: C, 52.79; H, 5.36; N, 9.72. Found: C, 52.94; H, 5.02; N, 9.59. The $^{18}O_2$ analogue of the 1:2 adduct was prepared on a milligram scale by using the same method.

The gases $^{16}O_2$ (99.99%, Matheson), $^{18}O_2$ (99.89%, Monsanto Research), and Ar (99.9995%, Matheson) were used without further purification. All solvents were dried by refluxing over CaH_2 and then distilled prior to use. Pyridine (py), aniline, benzylamine ($bzNH_2$), γ-picoline (γ-pic), *n*-butylamine (*n*-$BuNH_2$), and 1-methylimidazole (1-MeIm) were dried over NaOH and distilled before use. 4-Cyanopyridine (CN-py) was recrystallized from hexane. Triphenylphosphine (PPh_3), tributylphosphine (PBu_3), and methyl isonicotinate (Me-*i*-nic) were used without further purification. All bases were purchased from Aldrich Chem. Co., Milwaukee, WI.

Spectral Measurements. The "base-free" Co(J-en)O_2 was prepared by using the matrix cocondensation techniques: Co(J-en) was vaporized from a Knudsen cell at ~430 K and cocondensed with $^{16}O_2$ or $^{18}O_2$ on a CsI window that was cooled to ~16 K by a CTI Model 21 closed-cycle helium refrigerator. IR spectra were measured on a Beckman 4260 infrared spectrophotometer with a 25 cm^{-1}/in. chart expansion and 5

* Marquette University.

(1) Carter, M. J.; Rillema, D. P.; Basolo, F. *J. Am. Chem. Soc.* **1974**, *96*, 392.
(2) Kozuka, M.; Nakamoto, K. *J. Am. Chem. Soc.* **1981**, *103*, 2162.
(3) Urban, M. W.; Nonaka, Y.; Nakamoto, K. *Inorg. Chem.* **1982**, *21*, 1046.
(4) Jones, R. D.; Budge, J. R.; Ellis, P. E., Jr.; Linard, J. E.; Summerville, D. A.; Basolo, F. *J. Organo. Met. Chem.* **1979**, *181*, 151.
(5) Kubokura, K.; Okawa, H.; Kida, S. *Bull. Chem. Soc. Jpn.* **1978**, *51*, 2036.

0002-7863/82/1504-3386$01.25/0 © 1982 American Chemical Society

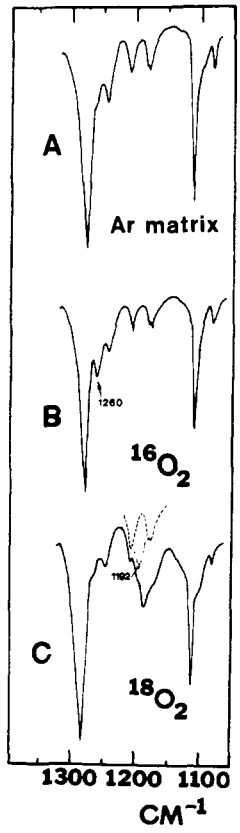

Figure 1. IR spectra of Co(J-en): (A) in an Ar matrix, (B) in a pure $^{16}O_2$ matrix, and (C) in a pure $^{18}O_2$ matrix (all at ~16 K).

cm^{-1}/min chart speed. Rotation–vibration bands of standard molecules and polystyrene film bands were used for calibration of frequency reading.

RR spectra of solutions containing Co(J-en) and a base ligand were measured in a Dewar cell designed in our laboratory. In a typical experiment, ca. 2 mmol of Co(J-en) was dissolved in 10 mL of CH_2Cl_2 containing 3% base ligand under nitrogen atmosphere. The solution was cooled with a 1,2-dichloroethane slush (−35 °C) or dry ice–acetone (−78 °C) and degassed by evacuation of the cell. After evacuation, the solution was saturated with 1 atm of O_2 gas.

For the measurements of RR spectra of solutions at higher O_2 pressures and for the $^{18}O_2$ experiments, we devised the following technique. A solution of Co(J-en) (10^{-2} M) containing a base ligand was introduced into a small bulb (total volume, ca. 0.4 mL) by using a standard vacuum line. After the solution was frozen by liquid nitrogen, a small amount of $^{16}O_2$ or $^{18}O_2$ (ca. 0.7 mL at 1 atm) was added, and the bulb was sealed off (**Caution**: The bulb may explode at ambient temperature due to the higher O_2 pressure (estimated to be ca. 3 atm)). This minibulb was attached to the front edge of the cold tip cooled by a CTI Model 21 closed-cycle helium refrigerator. Approximate temperatures in the bulb were estimated by the relative intensities of Stokes and anti-Stokes lines of CH_2Cl_2 measured under the same experimental conditions. To plot the excitation profiles, we measured relative intensities of $\nu(O_2)$ against the 918-cm^{-1} band of the solvent (CH_3CN) and corrected for spectrometer sensitivity and the ν^4 law.

The RR spectra of the 1:2 adduct in the solid state were measrued as pellets containing K_2SO_4. To avoid the rapid exchange of $^{16}O_2$–$^{18}O_2$ in the air, we measured the RR spectrum of the $^{18}O_2$ analogue under vacuum at ca. −120 °C.[7]

The RR spectra were recorded on a Spex Model 1401 double monochromator with a Spex digital photometer system. Excitations at 457.9, 476.5, 488.0, 496.5, and 514.5 nm were made with a Spectra-Physics Model 164 Ar-ion laser. Excitations in the 540–600-nm region were made by a Spectra-Physics Model 365 dye-laser (Rhodamine 6G and sodium fluorescein) pumped by the above Ar-ion laser. The 647.1-nm line was provided by a Spectra-Physics Model 165 Kr-ion laser at Northwestern University. Calibrations of frequency readings were made by using plasma lines from the Ar-ion laser.

A Cary Model 14 UV–visible spectrophotometer was used to measure the electronic spectra of molecular oxygen adducts of Co(J-en) in solution which were cooled to −35 °C in a Dewar cell.

Table I. In-Plane Ligand Effect on O_2 Stretching Frequencies (cm^{-1})

	$\nu(^{16}O_2)$	$\nu(^{18}O_2)$	shift[a]
$Co(TPP)O_2$[b]	1278	1209	69
$Co(J\text{-}en)O_2$	1260	1192	68
$Co(acacen)O_2$[c]	1146	1098	48

[a] Isotope shift, $\nu(^{16}O_2) - \nu(^{18}O_2)$. [b] Reference 2. [c] Reference 3.

Results and Discussion

Infrared Spectrum of Co(J-en)O_2. Trace A of Figure 1 shows the IR spectrum of Co(J-en) in an Ar matrix at ~16 K. No new bands were observed when Co(J-en) was codeposited with $^{16}O_2$ diluted in Ar at ~16 K. A new band appeared at 1260 cm^{-1}, however, when pure $^{16}O_2$ gas was used as a matrix (trace B). This band disappeared and a broad band centered at ~1180 cm^{-1} appeared in pure $^{18}O_2$ matrix (trace C). Subtraction of the Co(J-en) spectrum (trace A) from trace C revealed the presence of a new band at 1192 cm^{-1}, as shown by the dotted line in trace C. Thus, the bands at 1260 and 1192 cm^{-1} have been assigned to the $\nu(^{16}O_2)$ and $\nu(^{18}O_2)$ of Co(J-en)O_2, respectively. Previously, we were able to assign an asymmetric end-on structure for the Co-O_2 moiety of Co(TPP)O_2 based on isotope scrambling experiments.[2] No such attempts were made for Co(J-en)O_2 due to serious overlap of its $\nu(O_2)$ with Co(J-en) bands.

Table I summarizes the $\nu(O_2)$ of three "base-free" Co(II) chelate–O_2 adducts. It is seen that the order of $\nu(O_2)$ is Co(TPP)O_2 > Co(J-en)O_2 ≫ Co(acacen)O_2. Previously, Carter et al.[1] observed that the redox potential for Co(II) → Co(III) ($-E_{1/2}$, V, vs. SCE) increases markedly in going from Co(p-MeOTPP)py (−0.23) to Co(acacen)py (−0.59). This result suggests that the electron density on the Co atom is much less in the former than in the latter. Apparently, *p*-MeOTPP delocalizes more electrons from the Co into the ligand π system than acacen. A larger electron density on Co facilitates electron donation from the Co to the O_2, resulting in a lower $\nu(O_2)$. Thus, the above order of $\nu(O_2)$ suggests that the in-plane ligand effect of J-en is close to that of TPP due to the strong electron-withdrawing effect of its acetyl group.

Resonance Raman Spectra of O_2 Adducts in Solution. The following equilibria are established when Co(J-en) in CH_2Cl_2 or CH_3CN absorbs oxygen in the presence of a base (B) at low temperatures:

$$\text{Co(J-en)B} + O_2 \overset{K_1}{\rightleftharpoons} \text{Co(J-en)BO}_2 \quad (1)$$

$$\text{Co(J-en)BO}_2 + \text{Co(J-en)B} \overset{K_2}{\rightleftharpoons} [\text{Co(J-en)B}]_2O_2 \quad (2)$$

As reported in our previous communication,[8] it is possible to observe the $\nu(O_2)$ of both 1:1 and 1:2 adducts simultaneously and to study the effects of the axial ligand (B), temperature, O_2 pressure, and solvent polarity on such equilibria by using RR spectroscopy. Although UV–visible spectroscopy was used previously[1,9] to determine the equilibrium constant for eq 1, it is difficult to apply this method to a solution containing both adducts since their electronic spectra tend to overlap. In contrast, the $\nu(O_2)$ of the 1:1 and 1:2 adducts appear in distinctly different regions: 1280–1000 cm^{-1} for the former and 910–800 cm^{-1} for the latter.[2,3,7,8]

Trace A of Figure 2 shows the RR spectrum (580-nm excitation) of Co(J-en) in CH_3CN containing 3% pyridne which was saturated with $^{16}O_2$ at −35 °C. The strong band at 918 cm^{-1} is

(6) Nishida, Y.; Kida, S.; Cremer, S.; Nakamoto, K. *Inorg. Chim. Acta* **1981**, *49*, 85.
(7) Suzuki, M.; Ishiguro, T.; Kozuka, M.; Nakamoto, K. *Inorg. Chem.* **1981**, *20*, 1993.
(8) Kozuka, M.; Suzuki, M.; Nishida, Y.; Kida, S.; Nakamoto, K. *Inorg. Chim. Acta* **1980**, *45*, L111.
(9) Stynes, D. V.; Stynes, H. C.; Ibers, J. A.; James, B. R. *J. Am. Chem. Soc.* **1973**, *95*, 1142.

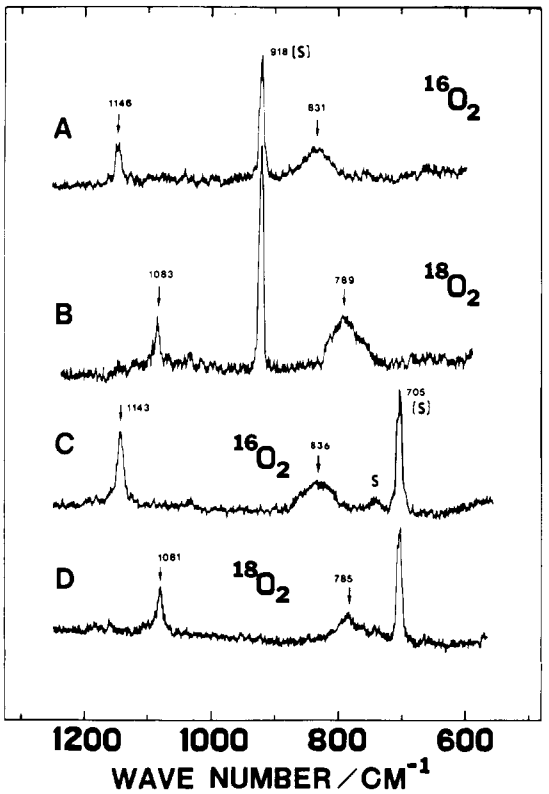

Figure 2. RR spectra of Co(J-en) in CH_3CN or CH_2Cl_2 containing 3% pyridine (580-nm excitation): (A) CH_3CN, saturated with $^{16}O_2$ at -35 °C, (B) CH_3CN, saturated with $^{18}O_2$ at -35 °C, (C) CH_2Cl_2, saturated with $^{16}O_2$ at -78 °C, and (D) CH_2Cl_2, saturated with $^{18}O_2$ at -78 °C. S denotes solvent bands.

due to the solvent. Two bands at 1146 and 831 cm^{-1} can be assigned to the $\nu(O_2)$ of the 1:1 and 1:2 adducts, respectively, since they are shifted to 1083 and 789 cm^{-1}, respectively, by $^{16}O_2$–$^{18}O_2$ substitution (trace B) and since they do not appear in the absence of oxygen. Trace C shows the RR spectrum of Co(J-en) in CH_2Cl_2 containing 3% pyridine which was saturated with $^{16}O_2$ at −78 °C. The strong band at 705 cm^{-1} and a weak band near 720 cm^{-1} are due to the solvent. Again the bands at 1143 and 836 cm^{-1} are assigned to the $\nu(O_2)$ of the 1:1 and 1:2 adducts, respectively, since they are shifted to 1081 and 785 cm^{-1}, respectively, by $^{16}O_2$–$^{18}O_2$ substitution (trace D). These $\nu(O_2)$ bands were used to study the effects of O_2 pressure, temperature, solvent polarity, and basicity of the axial ligand on the solution equilibria.

(A) Effect of O_2 Pressure. Traces A and B of Figure 3 compare the RR spectra of Co(J-en) in CH_2Cl_2 containing 3% pyridine at −80 °C under 1 and ca. 3 atm O_2 pressures, respectively (580-nm excitation). It is seen that the 1:1 adduct peak at 1143 cm^{-1} becomes stronger and the 1:2 adduct peak at 836 cm^{-1} becomes weaker as the O_2 pressure increases. Thus, the formation of the 1:1 adduct is favored at a higher O_2 pressure. This is expected from equilibrium 1 as well as from equilibrium 3.

$$[\text{Co(J-en)B}]_2O_2 + O_2 \underset{}{\overset{K_1/K_2}{\rightleftharpoons}} 2\text{Co(J-en)BO}_2 \qquad (3)$$

(B) Effect of Temperature. Traces B, C, and D of Figure 3 show the RR spectra of Co(J-en) in CH_2Cl_2 containing 3% pyridine at -80, -30, and +20 °C, respectively (580-nm excitation). It is seen that the 1:1 adduct peak at 1143 cm^{-1} becomes weaker and the 1:2 adduct peak at 836 cm^{-1} becomes stronger as the temperature is raised from -80 to +20 °C. The observed spectral changes are reversible within this temperature range. Previously, Stynes et al.[9] obtained thermodynamic and kinetic data for equilibrium 1 involving cobalt(II) protoporphyrin IX dimethyl ester and Carter et al.[1] reported thermodynamic data for the same equilibrium involving several Co(II) Schiff base complexes. However, no such data were obtained for equilibrium 2 because the electronic spectra of the 1:1 and 1:2 adducts overlap.

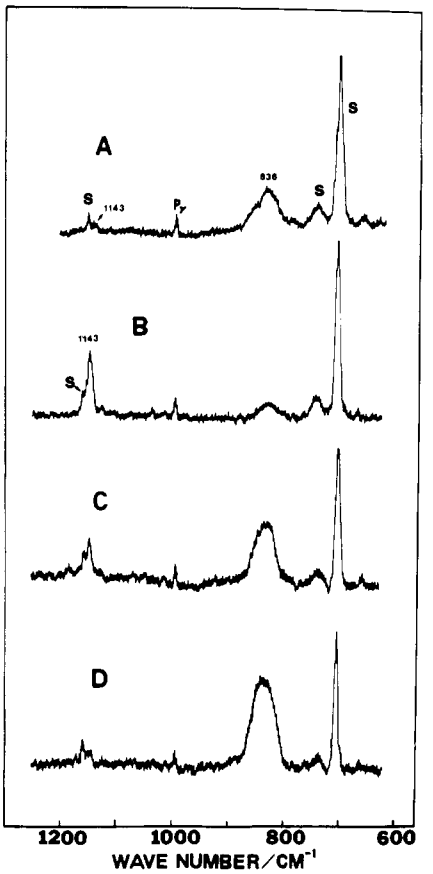

Figure 3. RR spectra of Co(J-en) in CH_2Cl_2 containing 3% pyridine which were saturated with O_2 at various O_2 pressures and temperatures (580 nm-excitation): (A) 1 atm, −78 °C, (B) ~3 atm, −80 °C, (C) ~3 atm, −30 °C, and (D) ~3 atm, +20 °C. S and py denote the solvent and pyridine bands, respectively.

The relative concentration of the 1:1 and 1:2 adducts at temperature T_1 is given by

$$\frac{\{[\text{Co(J-en)B}]_2O_2\}}{\{\text{Co(J-en)BO}_2\}^2} = \frac{K_2(T_1)}{K_1(T_1)} \frac{1}{[O_2]_{T_1}} \qquad (4)$$

Here, braces indicate the concentratons of the adducts. At T_2, the relative concentration is expressed as

$$\frac{\{[\text{Co(J-en)B}]_2O_2\}}{\{\text{Co(J-en)BO}_2\}^2} = \frac{K_2(T_1)}{K_1(T_1)} \frac{1}{[O_2]_{T_2}} \exp\left(\frac{(\Delta H_2 - \Delta H_1)(T_2 - T_1)}{RT_2T_1}\right) \qquad (5)$$

If T_1 and T_2 are 293 and 193 K, respectively, then, $T_2 - T_1 <$ O. The results shown in Figure 3 (traces B, C, and D) indicate that, in going from T_1 to T_2, the concentration of the 1:1 adduct increases and that of the 1:2 adduct decreases. This implies that the term, $\Delta H_2 - \Delta H_1$, must be positive. Namely, the second reaction must be less exothermic than the first reaction.

In the above discussion, we have assumed that $[O_2]_{T_1} \simeq [O_2]_{T_2}$. In practice, $[O_2]_{T_1} > [O_2]_{T_2}$ since our experiments were carried out for a solution sealed in a minibulb. As discussed in the preceding section, the 1:1 adduct formation is favored at a lower temperature. Apparently, the O_2 pressure effect was insufficient to offset the temperature effect under our experimental conditions.

(C) Solvent Polarity. Traces A and B of Figure 4 show the RR spectra (580-nm excitation) of Co(J-en) in CH_3CN containing 3% PPh_3 at −35 °C which were saturated with $^{16}O_2$ and $^{18}O_2$, respectively. The band at 1140 cm^{-1} is due to the 1:1 adduct since it shifts to 1073 cm^{-1} by $^{16}O_2$–$^{18}O_2$ substitution. Traces C and D are the RR spectra of Co(J-en) in CH_2Cl_2 containing 3% PPh_3 at −78 °C which were saturated with $^{16}O_2$ and $^{18}O_2$, re-

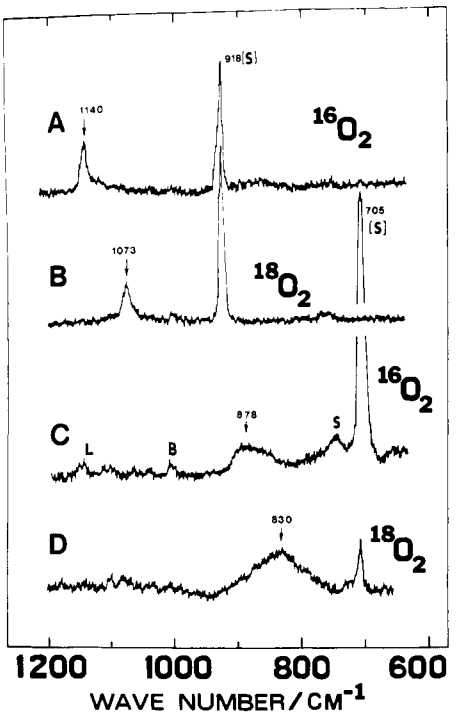

Figure 4. RR spectra of Co(J-en) in CH_3CN (traces A and B) containing 3% PPh_3 at −35 °C and in CH_2Cl_2 (traces C and D) containing 3% PPh_3 at −78 °C (580 nm). Traces A and C are those saturated with $^{16}O_2$, and traces B and D are those saturated with $^{18}O_2$. S, B, and L denote peaks due to the solvent, base, and Co(J-en), respectively.

spectively. The band at 878 cm^{-1} is due to the 1:2 adduct since it shifts to 830 cm^{-1} by $^{16}O_2$–$^{18}O_2$ substitution. It should be noted that traces A and B (CH_3CN, −35 °C) show only the 1:1 adduct bands while traces C and D (CH_2Cl_2, −78 °C) show only the 1:2 adduct bands. Since the dipole moments of CH_3CN and CH_2Cl_2 are 3.97 and 1.54 D, respectively, the above results indicate that the 1:1 adduct is stabilized in a polar solvent such as CH_3CN, whereas the 1:2 adduct is stabilized in a less polar solvent such as CH_2Cl_2. Apparently, this polarity effect is dominant over the temperature effect discussed above, since traces A and B were obtained at −35 °C whereas those of C and D were obtained at −78 °C. In general, the Co(II)–O_2 bond is regarded as a polar superoxo Co(III)–O_2^- type,[10] which means that its formation from the less polar reactants is enhanced by polar solvents. The opposite trend observed for the 1:2 adduct seems to suggest that the overall polarity of the 1:2 adduct is small due to cancellation of two Co(III)–O_2^- bond moments in the μ-peroxo bridged structure, Co(III)–O_2^{2-}–Co(III).

(D) Effect of Axial Ligands. As demonstrated previously, coordination of a base to "base-free" adduct causes a marked shift of $\nu(O_2)$ to a lower frequency: Co(TPP)O_2 (1278)[2] to Co(TPP)(1-MeIm)O_2 (1142),[4] Co(acacen)O_2 (1146) to Co(acacen)(py)O_2 (1025),[3] [Co(salen)]$_2O_2$ (1011)[7] to [Co(salen)(py)]$_2O_2$ (888)[11] (all in units of cm^{-1}). A similar large shift is expected when Co(J-en)O_2 is coordinated by a basic ligand. Much smaller shifts of $\nu(O_2)$ are anticipated, however, when the ligand is varied in a series of a 1:1 or 1:2 adducts.

Figure 5 shows the RR spectra of Co(J-en) in CH_2Cl_2 containing a variety of axial ligands which are saturated with $^{16}O_2$ and measured at −78 °C (580-nm excitation). Similar experiments were carried out in CH_3CN at −35 °C. Table II lists all the $\nu(O_2)$ of the 1:1 and 1:2 adducts observed. It is seen that no 1:1 adduct bands were observed with N-base ligands of pK_a below 5.0. This result clearly indicates that formation of the 1:1 adduct is favored in the presence of a stronger base.

(10) Jones, R. D.; Summerville, D. A.; Basolo, F. *Chem. Rev.* **1979**, *79*, 139.

(11) Nakamoto, K.; Suzuki, M.; Ishiguro, T.; Kozuka, M.; Nishida, Y.; Kida, S. *Inorg. Chem.* **1980**, *19*, 2822.

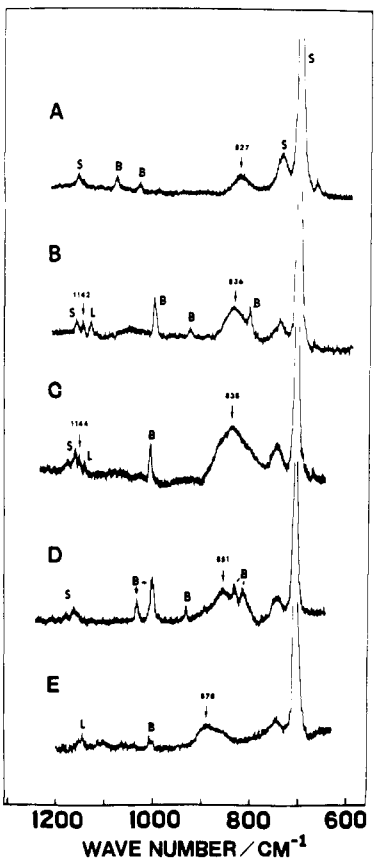

Figure 5. RR spectra of Co(J-en) in CH_2Cl_2 containing a variety of axial ligands (580 nm), all saturated with $^{16}O_2$ and measured at -78 °C: (A) 1-MeIm, (B) γ-pic, (C) $bzNH_2$, (D) aniline, and (E) PPh_3. S, B, and L denote peaks due to the solvent, base, and Co(J-en), respectively.

Table II. O_2 Stretching Frequencies (cm^{-1}) of 1:1 and 1:2 O_2 Adducts of Co(J-en) Containing a Variety of Base Ligands

			CH_2Cl_2, −78 °C		CH_3CN, −35 °C	
no.[a]	base	pK_a[b]	1:2	1:1	1:2	1:1
1	1-MeIm	7.20	827	1145	823	1146
2	γ-pic	6.02	836	1142	828	1145
3	py	5.20	836	1143	831	1146
4	Me-*i*-nic	3.26	838		*c*	*c*
5	CN-py	1.85	840		*c*	*c*
6	*n*-$BuNH_2$	10.61	835	1143	830	1143
7	$bzNH_2$	9.33	838	1144	820	1143
8	aniline	4.60	851		850	
9	PBu_3	8.43	839	1136	835	1134
10	PPh_3	2.73	878			1140

[a] These numbers are referred to Figure 6. [b] pK_a of the conjugated acid of a base. [c] Precipitation occurs due to low solubility of the adduct.

Table II also shows that, for the N-base ligands, the $\nu(O_2)$ of the 1:1 adducts are in a narrow range from 1146 to 1142 cm^{-1} whereas those of the 1:2 adducts are in a wide range from 851 to 820 cm^{-1}. An opposite trend was found previously for the Co(acacen) series: the $\nu(O_2)$ of the 1:1 adducts ranges from 1025 (py) to 1003 (*n*–$BuNH_2$), and that of the 1:2 adducts spans over the range from 808 (py) to 798 cm^{-1} (*n*-$BuNH_2$).[3] Thus, the $\nu(O_2)$ of 1:1 and 1:2 adducts exhibit different "base–ligand sensitivities" depending upon the nature of the in-plane chelating ligand. More experimental data are necessary before a general statement can be made regarding the reasons for this behavior.

Figure 6 plots the $\nu(O_2)$ of the 1:2 adducts against the pK_a of the axial ligand. In general, the $\nu(O_2)$ shifts to a lower frequency as the pK_a of the axial ligand increases. However, group A (γ-pic, py, Me-*i*-nic, and CN-py) give a straight line which is lower in the ordinate scale than that obtained for group B ligands (*n*-

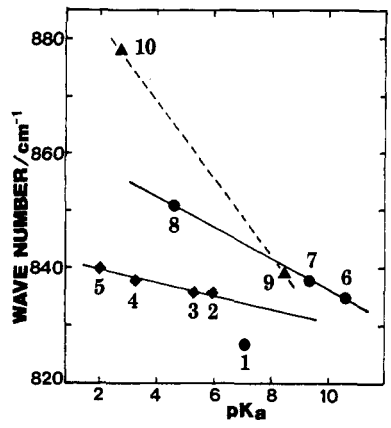

Figure 6. A plot of $\nu(O_2)$ of $[Co(J\text{-en})(B)]_2O_2$ vs. pK_a of the conjugated acid of a base (B). The numbers refer to the designation of the base given in Table II.

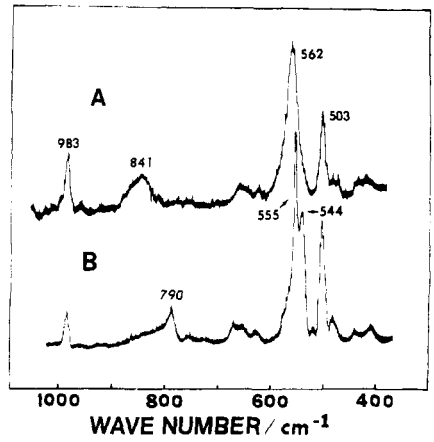

Figure 7. RR spectra of solid $[Co(J\text{-en})(py)]_2O_2$ obtained by the 587-nm excitation at ~150K: (A) $^{16}O_2$ adduct, (B) $^{18}O_2$ adduct. The 983-cm^{-1} band is due to K_2SO_4 (internal standard).

$BuNH_2$, $bzNH_2$, and aniline). This difference may be attributed to the effect of π basicity on the $\nu(O_2)$ since groups A and B are regarded as $\sigma + \pi$ and pure σ donors, respectively. The $\nu(O_2)$ of 1-MeIm shows a deviation from the straight line for group A. This is not unexpected since imidazoles are much better π donors than pyridines.[10]

An unusually high $\nu(O_2)$ (878 cm^{-1}) was observed when PPh_3 was used as an axial ligand. This is understandable since it has a small pK_a value (2.73) and is known as a good π acceptor. However, PBu_3 behaves like a group A base because substitution of the phenyl by the butyl group increases the pK_a value and diminishes the π acceptor ability. Attempts to confirm a straight-line relationship for a series of phosphine ligands failed since intermediate ligands such as PPh_2Bu and $PPhBu_2$ gave extremely unstable products.

Resonance Raman Spectra of $[Co(J\text{-en})(py)]_2O_2$ in the Solid State. As stated in the Experimental Section, the microanalytical results on black-purple crystals obtained from the reaction of Co(J-en) with O_2 in toluene containing 5% pyridine conform to the formula $[Co(J\text{-en})(py)]_2O_2$. This is further confirmed by its RR spectra shown in Figure 7; trace A shows a band at 841 cm^{-1}, which is shifted to 790 cm^{-1} by $^{16}O_2$–$^{18}O_2$ substitution (trace B). Thus, the 841-cm^{-1} band must be assigned to the $\nu(O_2)$ of the above 1:2 adduct. Previously, this compound was thought to be a 1:1 adduct.[5] However, both RR spectra and microanalytical results clearly indicate that it is a 1:2 adduct of the above formula.

The band at 562 cm^{-1} (trace A) has been assigned to the symmetric Co–O stretching vibration, $\nu_s(CoO)$, for the following reasons: (1) This band shifts to 544 cm^{-1} by $^{16}O_2$–$^{18}O_2$ substitution (trace B). The magnitude of this shift (18 cm^{-1}) is comparable to that observed for the $\nu_s(CoO)$ of $[Co(salen)]_2O_2$ (17 cm^{-1}).[7] (2) $[Co(salen)(pyO)]_2O_2$ and $[Co(salen)(py)]_2O_2$ exhibit similar

Table III. O_2 and CoO Stretching Frequencies of 1:2 (O_2/Co) Adducts (cm^{-1})

no.[a]	compd	$\nu(O_2)$	$\nu_s(CoO)$	ref
1	$[Co(salen)]_2O_2$	1011	533	7
2	$[Co(salen)(pyO)]_2O_2$	910	535	11
3	$[Co(salen)(py)]_2O_2$	888	542	11
4	$[Co(J\text{-en})(py)]_2O_2$	841	562	*b*
5	$[Co(L\text{-his})_2]_2O_2$	811	600	12
6	$[\{Co(NH_3)_5\}_2O_2](NO_3)_4$	805	642	13

[a] Refer to Fig. 8. [b] Present work.

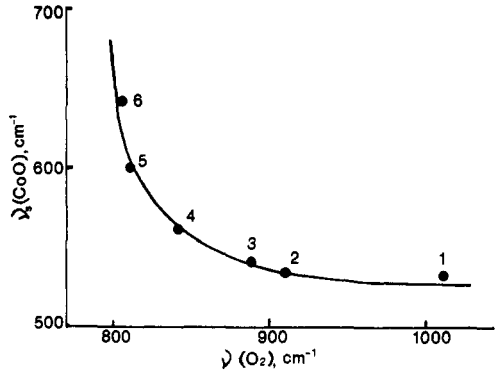

Figure 8. Plot of $\nu(O_2)$ vs. $\nu_s(CoO)$ for 1:2 (O_2/Co) adducts.

bands at 535 and 542 cm^{-1}, respectively.[10] (3) The relative intensities of both bands at 841 and 562 cm^{-1} increase as the laser wavelength becomes closer to 610 nm where the Co–O_2 CT band of the 1:2 adduct is expected (Figure 9). Although the 503-cm^{-1} band also shows a similar intensity variation, it is not sensitive to $^{16}O_2$–$^{18}O_2$ substitution and is probably due to a skeletal vibration of the CoN_2O_2 core.

Table III lists the $\nu(O_2)$ and $\nu_s(CoO)$ of six 1:2 adducts for which definitive assignments are available. A plot of $\nu(O_2)$ vs. $\nu_s(CoO)$ shown in Figure 8 indicates that $\nu_s(CoO)$ is approximately proportional to the reciprocal of the square of $\nu(O_2)$. We have shown previously that the $\nu(O_2)$ shifts to a lower frequency as the negative charge on the O_2 increases.[3,6-8] Thus, the present results suggest that an increasing negative charge on the O_2 results in a stronger Co–O bond and a higher $\nu_s(CoO)$.

Electronic Spectra and Excitation Profiles of 1:1 and 1:2 Adducts. Electronic spectra of Co(II) Schiff base complexes consist of ligand π–π^*, ligand–metal π–d, metal–ligand d–π^*, and metal d–d transitions. Upon oxygenation, the color of the solution containing a Co(II) Schiff base complex is deepened. This deepening may be due to the emergence of a new Co–O_2 CT band or a shift of one of the above bands into the visible region. Previously, Kubokura et al.[5] measured the electronic spectra of Co(J-en) in dichloroethane containing pyridine at 0 °C as a function of the O_2 pressure and detected the appearance of a new, broad band at 525 nm which was attributed to the Co–O_2 CT bands of the 1:1 and 1:2 adducts. It was not possible, however, to separate these two bands or to confirm these assignments by electronic spectroscopy.

As stated previously, the $\nu(O_2)$ of the 1:1 and 1:2 adducts can be observed simultaneously in solution equilibria, and their intensities are expected to maximize when the laser frequency is tuned in the Co–O_2 CT energies of these adducts. Thus, RR spectroscopy provides a unique tool in locating these bands in solution equilibria containing both adducts.

The upper traces of Figure 9 show the electronic spectra of Co(J-en) in CH_3CN containing *n*-$BuNH_2$ saturated with N_2 (broken line) and O_2 (solid line) at −35 °C. It is seen that two new broad bands emerge at ca. 610 and 550 nm upon oxygenation of the solution. The lower traces of Figure 9 show the excitation profiles of the $\nu(O_2)$ of the 1:1 adduct at 1143 cm^{-1} and the 1:2

(12) Hester, R. E.; Nour, E. M. *J. Raman Spectrosco.* **1981**, *11*, 64.
(13) Shibahara, T.; Mori, M. *Bull. Chem. Soc. Jpn.* **1978**, *51*, 1374.

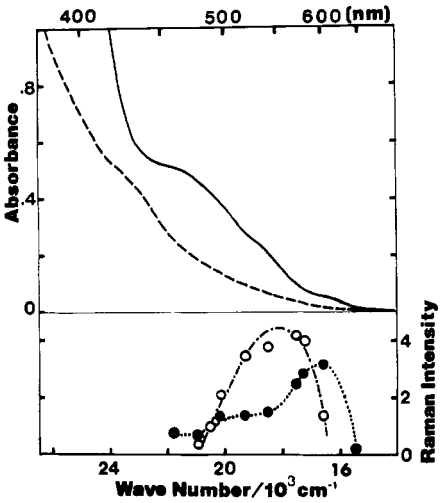

Figure 9. Electronic spectra and excitation profiles of Co(J-en)(*n*-$BuNH_2$)O_2 and [Co(J-en)(*n*-$BuNH_2$)]$_2O_2$ in CH_3CN(-35 °C). Upper curves: electronic spectra under N_2 (---) and O_2 (—) atmospheres (2 × 10^{-4} mol/L with respect to Co(J-en)). Lower curves: excitation profiles; ○, $\nu(O_2)$ of the 1:1 adduct; ●, $\nu(O_2)$ of the 1:2 adduct (10^{-2} mol/L with respect to Co(J-en)).

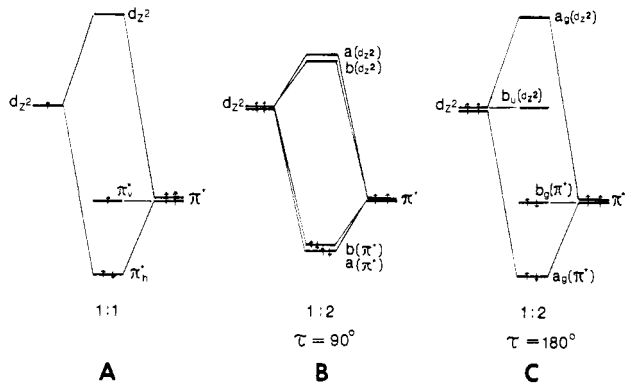

Figure 10. Schematic MO diagrams for the 1:1 and 1:2 adducts.

adduct at 830 cm^{-1} in CH_3CN containing 3% *n*-$BuNH_2$ at −35 °C. It is seen that the $\nu(O_2)$ of the former maximizes at ca. 550 nm whereas that of the latter maximizes at ca. 610 nm. These results strongly suggest that the electronic bands at 550 and 610 nm are due to the Co–O_2 CT transitions of the 1:1 and 1:2 adducts, respectively. Although the oxygenated solution exhibits another broad band at 525–475 nm, this band does not seem to contain Co–O_2 CT character since neither adduct shows resonance enhancement of the $\nu(O_2)$ when excited by the laser lines in this region.

Molecular Orbital Considerations. According to ab initio MO calculations on the 1:1 adduct Co(acacen)(B)O_2[14] the main bonding between the Co and O_2 occurs through the interaction of the d_{z^2} with the π_h* orbital (2pπ* orbital on the Co–O–O plane) (σ bonding). This results in two MOs, $\beta\pi^*_h + \alpha d_{z^2}$ and $\beta d_{z^2} - \alpha\pi^*_h$ ($\beta > \alpha$), which are abbreivated as the π^*_h and d_{z^2}, respectively, in Figure 10A. The energy of the π^*_v orbital (2pπ* orbital perpendicular to the Co–O–O plane) remains almost unchanged since its interaction with the dπ orbitals (π bonding) is rather weak.[14] Then, the transition of lowest energy should occur from the π^*_v to the d_{z^2} orbital. This transition may be responsible for the 550-nm band which causes resonance enhancement of the $\nu(O_2)$ of the 1:1 adduct.

Figure 10B shows a simple MO diagram used previously to account for the excitation profiles of the $\nu(O_2)$ and ν_s(CoO) of [Co(salen)(B)]$_2O_2$.[11] Its electronic band at ca. 500 nm has been attributed to the a(π*), b(π*) → a(d_{z^2}), b(d_{z^2}) transitions that accompany the Co–O_2 charge transfer. Here, a and b denote the orbitals which are symmetric and antisymmetric, respectively, with respect to the C_2 axis (the symmetry of the Co–O–O–Co skeleton is regarded as C_2 due to torsion about the O–O axis). The separation of the a and b orbitals is smallest when the torsional angle (τ) is 90° (Figure 10B) and largest when it is 180° (Figure 10C). According to X-ray analysis,[15] this angle is 110° for [Co(salen)(DMF)]$_2O_2$. Thus, Figure 10B represents an approximate MO diagram for the [Co(salen)(B)]$_2O_2$ type compounds.

When the torsional angle is 180° (C_{2h} symmetry), the π^*_v orbital (designated as $b_g(\pi^*)$) remains unchanged while the π^*_h orbital forms two MOs with the d_{z^2} orbital, which are designated as $a_g(\pi^*)$ and $a_g(d_{z^2})$ in Figure 10C. In this case, the Co–O_2 CT transition of the lowest energy may occur from the $b_g(\pi^*)$ to $b_u(d_{z^2})$ orbital. The observed red shift of the Co–O_2 CT band in going from [Co(salen)(B)]$_2O_2$ (500 nm) to [Co(J-en)(B)]$_2O_2$ (610 nm) may be accounted for if we assume that the torsional angle of the latter is much larger than that of the former. These MO schemes can also account for the observed trend in the $\nu(O_2)$ of the two compounds: the $\nu(O_2)$ of the latter (830 cm^{-1}) is lower than that of the former (890 cm^{-1}) because the two highest energy electrons in Figure 10C are in an orbital that is pure π^* while those in Figure 10B are in a mixed $d_{z^2} + \pi^*$ orbital. This torsional effect is somewhat compensated by the electron-withdrawing effect of the acetyl group in Co(J-en) since the latter lowers the d_{z^2} orbital and tends to decrease the electron density on the O_2. Apparently, the latter effect is superseded by the torsional effect in this case.

It is rather difficult to compare the Co–O_2 CT energies of the 1:1 and 1:2 adducts based on the rudimentary MO diagrams such as shown in Figure 10. In general, these energies depend upon relative energies of d_{z^2} and 2pπ* orbitals and the geometry of the Co–O_2 and Co–O_2–Co moieties, etc. In addition, one must consider the difference in electron repulsion energies between the 1:1 and 1:2 adducts. In the case of the 1:1 adduct, the transition occurs from the singly occupied π^*_v orbital. In the 1:2 adduct such as [Co(J-en)(B)]$_2O_2$, the transition may occur from the doubly occupied $b_g(\pi^*)$ orbital (figure 10C). Thus, the net Co–O_2 CT energy would be smaller by $J_{bb} - J_{bb'} - K_{bb'}$ than the orbital transition energy shown in Figure 10C. Here, $J_{bb} = \langle(b)(b)|(1/r_{12})|(b)(b)\rangle$, $J_{bb'} = \langle(b)(b')|(1/r_{12})|(b)(b')\rangle$, and $K_{bb'} = \langle(b)(b')|(1/r_{12})|(b')(b)\rangle$, where b and b′ denote the $b_g(\pi^*)$ and $b_u(d_{z^2})$ orbitals, respectively. Evidently, $J_{bb} - J_{bb'} - K_{bb'} > 0$, since $J_{bb} \gg J_{bb'} > K_{bb'}$: namely, the CT energy of the 1:2 adduct should be smaller by the spin pairing energy than that of the 1:1 adduct. This energy alone may account for the red shift of the Co–O_2 CT band of the 1:2 adduct relative to that of the 1:1 adduct.

It should be borne in mind that our schemes presented above are only tentative and cannot exclude alternative assignments such as those proposed by Lever and Gray.[16] More complete studies, both experimental and theoretical, are necessary to make unequivocal assignments of the electronic spectra of these O_2 adducts.

Acknowledgment. This work was supported by the National Science Foundation under Grant No. CHE-7915169. We thank Professor Fred Basolo and William C. Trogler of Northwestern University and Professor Dennis P. Strommen of Carthage College for their helpful discussions. Professor Duward F. Shriver of Northwestern University kindly allowed us to use his Kr-ion laser for the present work.

Registry No. Co(J-en), 63510-38-3; Co(J-en)O_2, 81340-40-1; Co(J-en)(1-MeIm)O_2, 81340-39-8; [Co(J-en)(1-MeIm)]$_2O_2$, 81360-29-4; Co(J-en)(γ-pic)]$_2O_2$, 81360-28-3; Co(J-en)(py)O_2, 67770-29-0; [Co(J-en)(py)]$_2O_2$, 67775-41-1; [Co(J-en)(Me-*i*-nic)]$_2O_2$, 81340-48-9; [Co(J-en)(CN-py)]$_2O_2$, 81340-47-8; Co(J-en)(*n*-$BuNH_2$)O_2, 81340-37-6; [Co(J-en)(*n*-$BuNH_2$)]$_2O_2$, 81340-46-7; Co(J-en)(bzNH_2)O_2, 81340-36-5; [Co(J-en)(bzNH_2)]$_2O_2$, 81340-45-6; [Co(J-en)(aniline)]$_2O_2$, 81340-44-5; Co(J-en)(PBu_3)O_2, 81360-43-2; [Co(J-en)(PBu_3)]$_2O_2$, 81340-43-4; [Co(J-en)(PPh_3)]$_2O_2$, 81340-42-3.

(14) Dedieu, A.; Rohmer, M. M.; Veillard, A. *J. Am. Chem. Soc.* **1976**, *98*, 5789.

(15) Galligaris, M.; Nardin, G.; Randaccio, L.; Ripamonti, A. *J. Chem. Soc.* **1970**, 1069.

(16) Lever, A. B. P.; Gray, H. B.; *Acc. Chem. Res.* **1978**, *11*, 348.